

The use of Synchronous Detection in Ultrasonic Flaw Detection of Large -Sized Products with Large Integral Attenuation of Signals

Vladimir K. Kachanov*, Igor V. Sokolov, Alexey A. Sinitsyn, Maksim B. Fedorov and Michael A. Karavaev

Moscow Power Engineering Institute (National Research University), Russia;
kachanovvk@mail.ru, sokoloff_igor@mail.ru, c.i.n@mail.ru, makstl@mail.ru, vezd@list.ru

Abstract

Background/Objectives: The use of simple radio-technical processing of signals – synchronous detection – in the ultrasonic testing of products with large frequency-dependent attenuation of ultrasound is considered. **Methods:** The use of radar in the ultrasonic flaw detection methods allows for control of objects with a high level of attenuation of ultrasonic vibrations in a material. **Findings:** It is demonstrated that synchronous detection increases the accuracy of echo signal temporal position measurement and increases the reliability of US testing in the presence of narrowband interference and the correlation with the probing signal of the electroacoustic pickup. **Improvements:** The use of synchronous detection will significantly increase the sensitivity and noise immunity of the ultrasound equipment used to control the complex structural materials with high attenuation of ultrasound, such as concrete, cast iron, plastic, etc.

Keywords: Ultrasonic Flaw Detection, Synchronous Detection, Optimal Filtering, Complex-Modulated Signals, Electroacoustic Pickup

1. Introduction

In most Ultrasonic (US) control devices, a simple unmodulated signal with duration of 1 to 2 periods of the carrier frequency is used as a probing signal. Thus, as a rule, no electro-technical processing of the US echo pulses is used. For this reason, on the screen of the indicator, we observe a US echo signal whose shape, without taking into account distortions in the Electroacoustic Tract (EAT), corresponds to the probing signal.

In recent years, products with a large integral attenuation of US signals to increase the sensitivity (for selection of US echo signals out of white noise), known from radio-location Frequency Modulated (FM) and Phase-Shift

Keyed (PSK) signals with subsequent optimal filtering of the echo signal, have been used. The shape of the signal at the output of the Optimal Filter (OF) is different from the input form of the signal:

$$S_1(j\omega) = |S_1(\omega)| \exp(j\varphi_c) \quad (1)$$

and it has the form:¹

$$U_2(t_0) = \frac{1}{2\delta} \int_{-\infty}^{\infty} |S_1(\dot{u})|^2 \cdot \dot{u} (j\dot{u}(t-t_0)) d\dot{u} = \dot{u} R(t_0) \quad (2)$$

*Author for correspondence

where ε - constant, and $R_0(t)$ is ACF of the signal:

$$R(t_0) = \frac{1}{2\pi} \int_{-\infty}^{\infty} |S_1(\omega)|^2 \cdot \exp(j\omega(t-t_0)) d\omega = \int_{-\infty}^{\infty} U_1(t) \cdot U_1(t-t_0) dt \quad (3)$$

In other words, the signal at the OF output $U_2(t_0)$ coincides in form with the Autocorrelation Function (ACF) of the signal. Taking into account that the signal energy is $A_1 = \frac{1}{2\pi} \int_{-\infty}^{+\infty} [S_1(\omega)]^2 d\omega$, from (2), we obtain for the

end of the signal $t = t_0 = T_s$; $U_2(t_0) \sim \varepsilon E_1$. Therefore, the OF output at the end of the pulse FM and PSK signals is not a temporary copy of the probing signal, and it has a type of ACF with one short maximum of duration $T_c \sim 1/\Delta f_s$ and low-level of side lobes. The amplitude of the peak is proportional to the signal energy, which, in turn, is determined by the duration of the complex-modulated signal T_s . For this reason, to ensure the high sensitivity of the US control, PSK and FM signals with a large duration (with a large base $B_s = T_s \Delta f_s = T_s/T_c \gg 1$) are selected, and to provide high-resolution capability, a wide band of signals Δf_c is provided.²

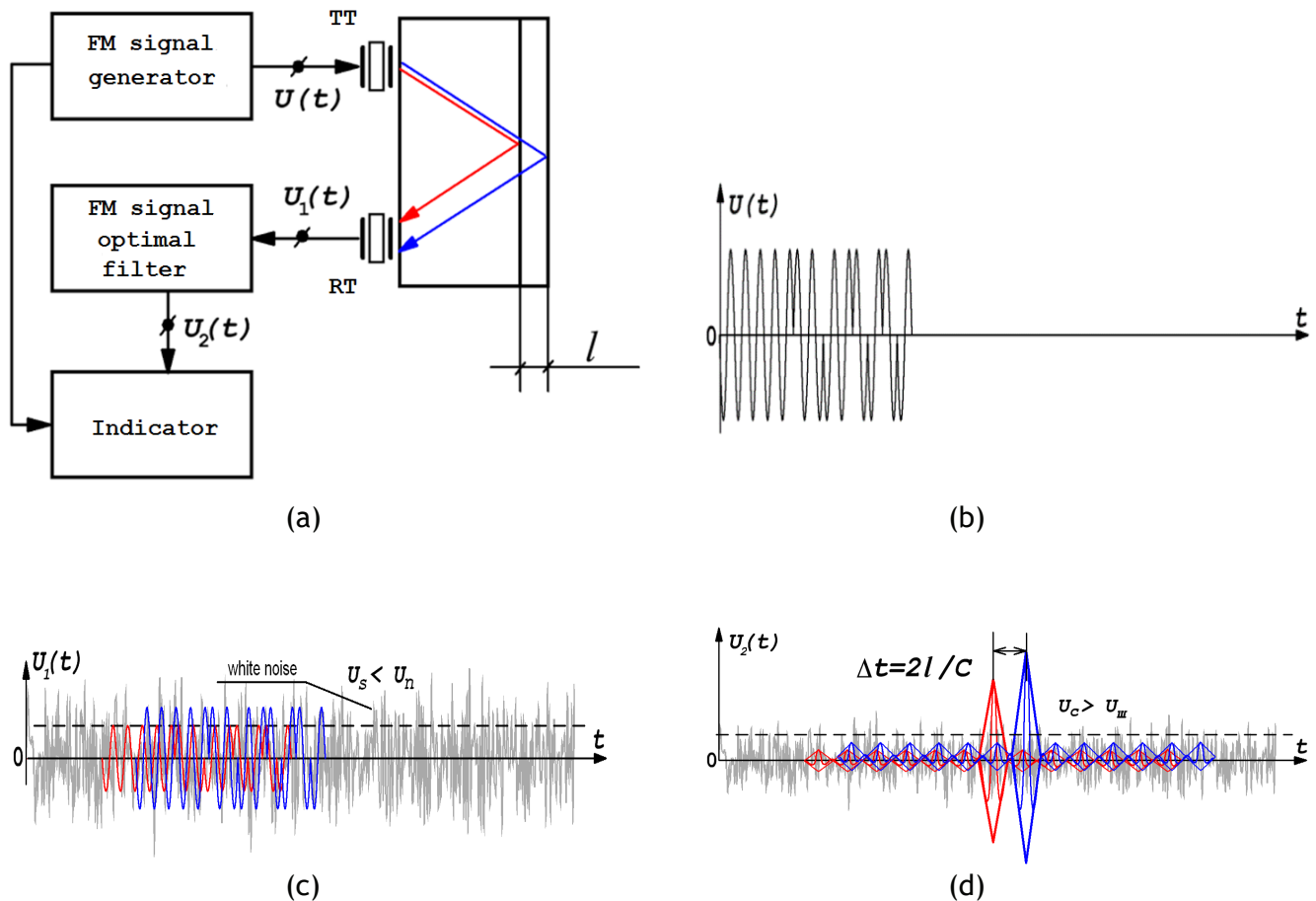


Figure 1. The main idea of using complex-modulated signals in US flaw detection to increase both the sensitivity and resolution capability of the echo control.

The application of complex-modulated signals solves the problem of the allocation of the echo signal from white noise (noise of receiving part of the US equipment), as well as the problem of simultaneously providing high values for the sensitivity and resolution capability of the control. The idea of increasing both the sensitivity and radial resolution capability of the US echo control is shown in Figure 1. In the product (Figure 1a), the long probing US PSK signal with the maximum amplitude (Figure 1b) is radiated. It is assumed that in a large-sized product with large integral attenuation, the US signals are attenuated so that the echo signals reflected from two defects located at a close distance l are not distinguished on the background of white noise (Figure 1c) because they are below the noise level of the receiving part of the equipment U_n . In addition, these echo signals are not resolved in time.

After passing through the optimal filter, the compressed signals are resolved in time and, by increasing the amplitude of the main lobe, are distinguished from noise (g). The temporal position of the echo signals is fixed by the positions of the maxima of the compressed pulses. This ensures high values of both the sensitivity and resolution capability.³

When using a non-modulated probe signal and when using complex-modulated signals and their subsequent compression in time in the optimal filter, the US echo signals are radio pulse, so it is not always possible to accurately determine their temporal positions. For this reason, it is advisable to view the control results in the form of a video pulse. In traditional flaw detection, conversion of a radio pulse into a video impulse is mainly carried out by means of amplitude detection, but the terms of the allocation of the US echo signals out of white noise when controlling products with a large signal attenuation require the use of synchronous detection of the echo signal because the synchronous detection does not deteriorate the signal/noise ratio.

2. Methods

The essence of synchronous detection is to transfer the signal spectrum in the region of the zero frequency, while the amplitude detection, the information contained in the phase of the signal, is stored, and the noise immunity of

the demodulation increases^{1,4}. The principle of the Synchronous Detector (SD), with some simplification, can be reduced to a multiplication of the input signal by a random initial phase $V_1 \cos(\omega_0 t + \varphi_1)$ on the reference

voltage, the frequency of which is strictly identical (synchronous) to the frequency of the input signal, with subsequent filtering of the high-frequency components in the Low-Pass Filter (LPF).

After multiplying, the result is a signal:

$$V_{\delta} = V_1 \cos(\omega_0 t + \varphi_1) V_{ref} \cos(\omega_0 t) = \frac{V_1 V_{ref}}{2} [\cos(2\omega_0 t + \varphi_1) + \cos \varphi_1] \tag{4}$$

At the output, the LPF signal does not contain the carrier frequency and has the form

$$V_{out} = \frac{V_1 V_{ref}}{2} \cos(\varphi_1) \tag{5}$$

Expression (5) defines the work of the device called the “phase detector”: the output voltage at the output of the phase detector is proportional to the input signal V_1 , the reference voltage V_{ref} and the cosine of the phase shift φ_1 between the input and reference signals. To eliminate uncertainty in the amplitude of the echo signal that arises due to the unknown initial phase of the signal, the diagram of the dual-channel quadrature processing shown in Figure 2, in which the signal processing with an initial phase of $V_1 \cos(\omega_0 t + \varphi)$ is conducted in two parallel chan-

nels with the reference signals $V_{ref} \cos(\omega_0 t)$ and $V_{ref} \sin(\omega_0 t)$, is used. After performing multiplication

and filtering in each channel, the signals are squared and then summed. The output signal at the output of the adder does not depend on the initial phase:

$$V_{out.S} = \left(\frac{V_1 V_{ref}}{2} \right)^2 (\sin^2 \varphi_1 + \cos^2 \varphi_1) = \left(\frac{V_1 V_{ref}}{2} \right)^2. \tag{6}$$

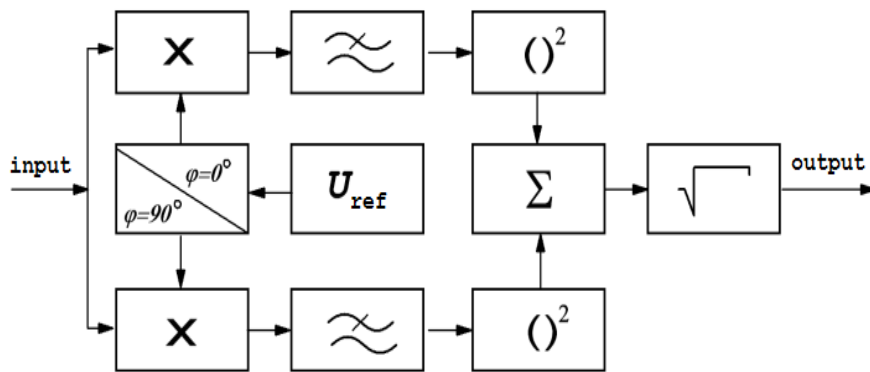


Figure 2. Structural diagram of two-channel synchronous receiver.

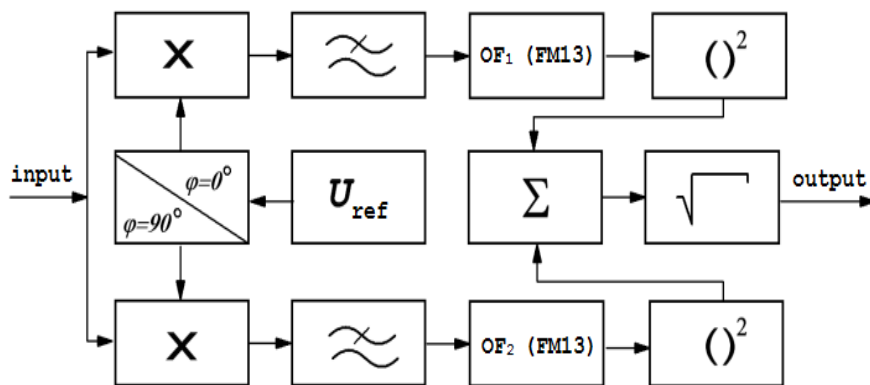


Figure 3. OF FM of Barker 13 signal with simultaneous detection and dual-channel quadrature processing.

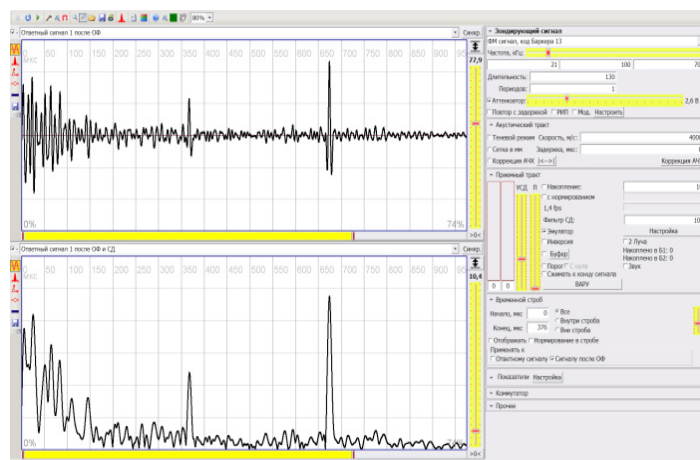


Figure 4. Results of US testing of the product with SM signal: at the top – the echo signal after OF; at the bottom – after OF and SD.

The signal after the scheme of the extraction of a square root is proportional to the input signal. Thus, during synchronous detection, the linear signal processing is in contrast to the amplitude detection. It is therefore easy to imagine a block diagram OF for the FM Barker 13 signal (3) where in each channel; there is an optimal filter for the Barker 13 video code.

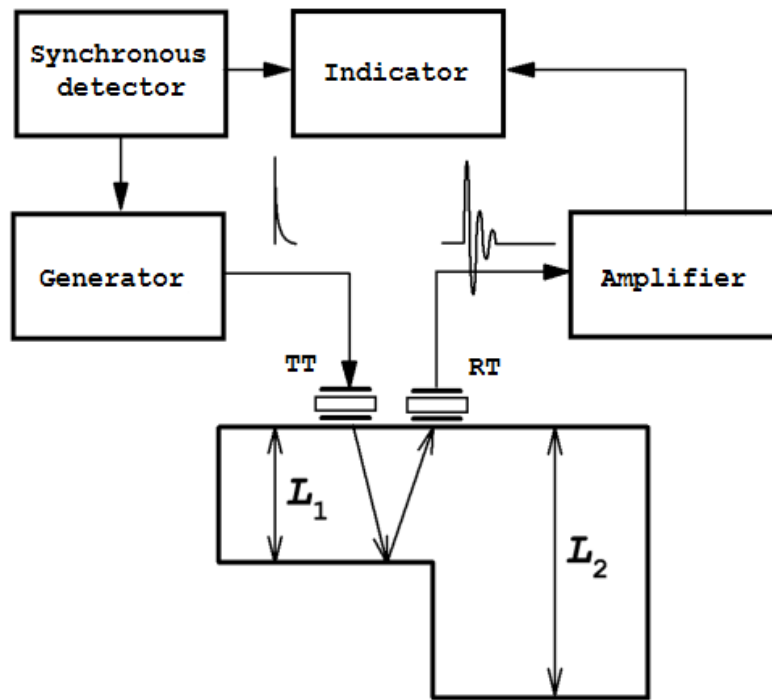
The effect of increasing the temporal position measurement accuracy of a complex-modulated echo signal is shown in Figure 4, which shows the results of the product control by the signal without synchronous detection of the echo signal (top) and after synchronous detection (bottom).

3. Results

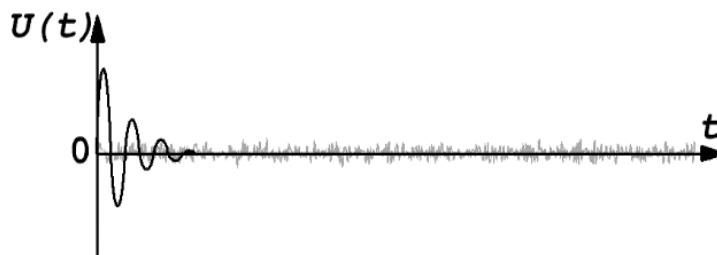
Figure 5 shows another application of the synchronous detector to reduce the measurement error of the echo signal temporal position.

Figure 5 shows a thickness measurement diagram for a product with thickness L_2 and an L_1 ($L_2 > L_1$) (Figure 5.a) short pulse (Figure 5b). In the thickness measurement of such products, the temporal position of the bottom echo signal is often determined by the crossing time of the echo signal of the threshold voltage $U_{threshold}$ (Figure 5c).

When measuring products of greater thickness L_2 , the amplitude of the echo signal is reduced, and the threshold



(a)



(b)

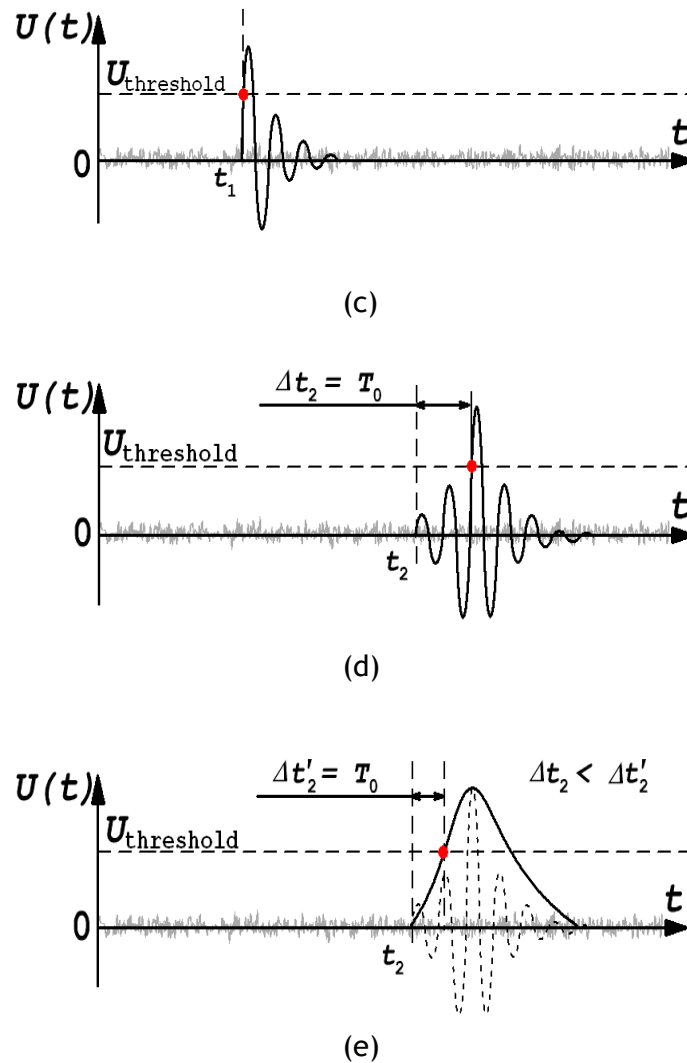


Figure 5. Forming errors $\delta\tau_1$ and $\delta\tau_2$ in US thickness measurement of products with a large attenuation of the echo signal. (a) - block diagram of the US echo pulse thickness measurement; (b) Probing signal; (c) echo signal from the defect at a depth of L1; (d) An echo from the defect at depth L2; (e) - echo signal after processing by the synchronous detector.

voltage is constant. In this case, the bottom echo signal may cross the threshold not at time t_2 , but at time $t_2 + T_0$ (Figure 5d), i.e., when measuring the temporal position of the echo signal, the error $\delta\tau_2$ is equal to the oscillation period of the probing signal T_0 (this effect is called the

“loss of period”). During strong attenuation of the echo signal, the error $\delta\tau_2$ may be equal to the length of two or three periods of the probing signal oscillation. The synchronous detection of the echo signal partially solves the

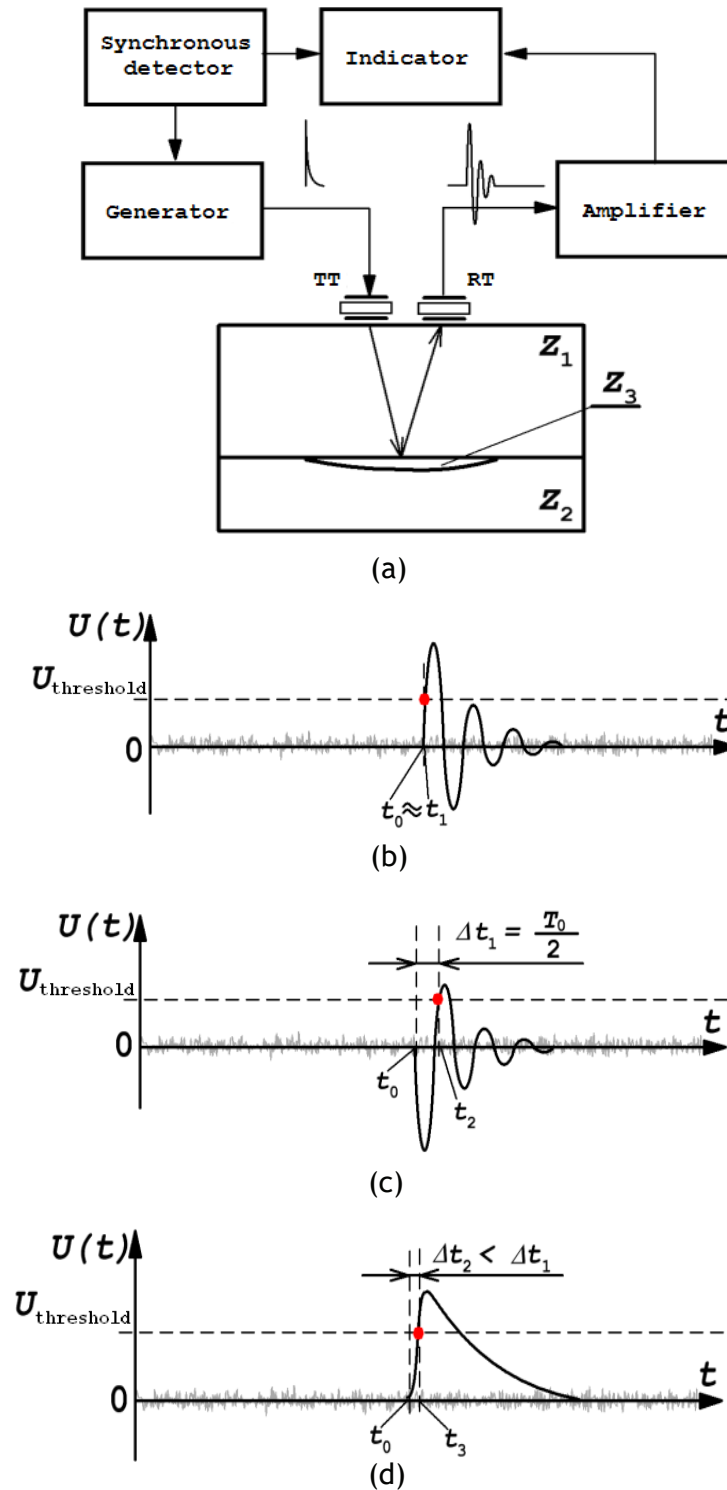


Figure 6. Error formation during the control of the layered products with acoustic impedance of layers Z_1 and Z_2 and a “defect” with acoustic impedance Z_3 ($Z_1 > Z_3$). (a-b) Probing signal; (c) Echo signal from the layer boundary Z_1 - Z_2 ; (d) echo signal from the layer boundary Z_1 - Z_3

problem of the “loss of period” and significantly reduces the thickness measurement error (see Figure 5e $\delta\tau_2 < \delta\tau_2$).

A similar example is shown in Figure 6. In the US thickness measurement of multilayer products or complex-structured products consisting of two or more fractions, it is possible that between two layers of the investigated material with an acoustic impedance Z_1-Z_2 , a foreign material (e.g., a crack filled with air from poor bonding of two layers) with an acoustic impedance Z_3 appears.

In the control of the layered product, the echo signal from the layer boundary Z_1-Z_2 is shown in Figure 6c. In the presence of the defect (in the case $Z_1 > Z_3$), the echo sig-

nal changes phase by 180° , and the error $\delta\tau = T_0/2$ (Figure 6d) – “loss of half-period” appears, which also leads to the error in the determination of the layer thickness.

4. Discussion

4.1 The Use of the Synchronous Detector for Extracting Signals from Narrowband Interference

Using the synchronous detection of the signals, it is possible to not only improve the accuracy of the measurement of

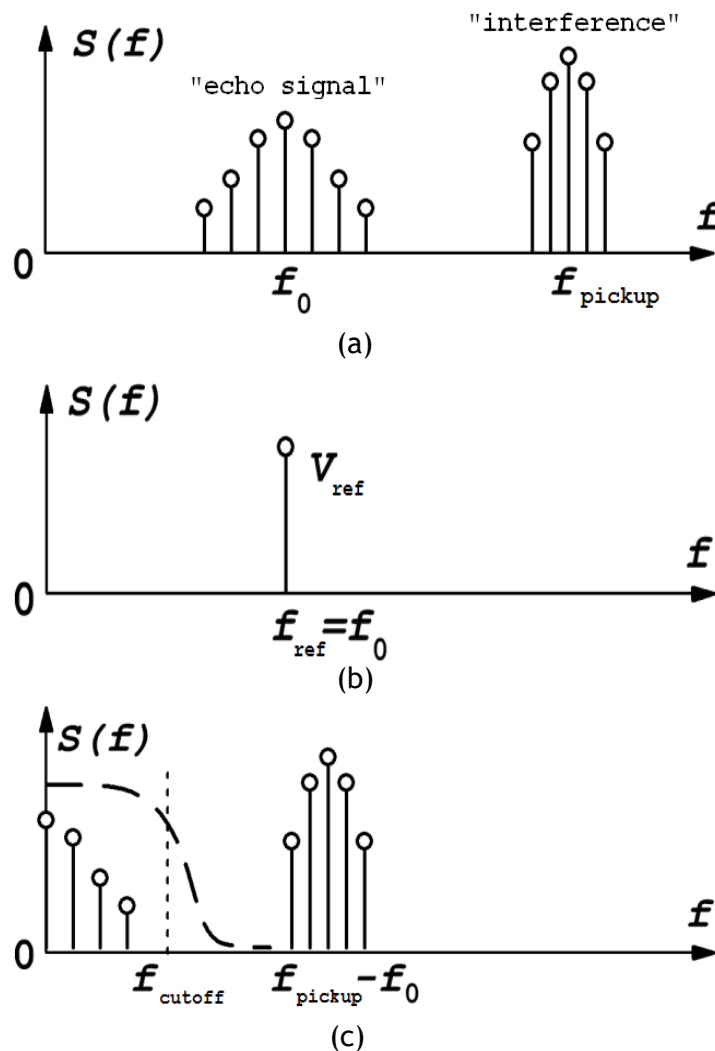


Figure 7. Application of SD to highlight the useful signal of the narrowband interference. (a) Signal and interference; (b) Reference signal f_0 ; (c) Signal at the SD output.

the echo signal, minimizing the measurement error, but in some cases, it is also possible to improve the noise immunity of the control⁴. Below, there is an example of the separation of a weak US signal from the narrow-band interference through the use of the dependence of the output signal of the synchronous detector from the amplitude of the reference signal (6).

SD “selectivity” allows selecting the echo signals whose frequency coincides with the frequency of the reference voltage and filter signals (interferences) with a different frequency f_n . An example of such a frequency separation of the signal and interference is shown in Figure 7, where the spectra of the signal and interference are given in Figure 7a, Figure 7b illustrates the spectral line of a reference oscillation with frequency $f_{ref}=f_o$, and Figure 7c shows the low-frequency components of the

signal spectrum and the spectrum of the interference after synchronous detection. If the cutoff frequency of the LPF in the synchronous detector is set so that $f_{cutoff} < (f_n - f_o)$, the suppression of the interference occurs. In the same Figure 7c, the effect of the conversion sensitivity increasing is observed: the amplitude of the spectral lines of the signal after detection exceeds the corresponding spectrum amplitudes before detection due to the multiplication of the amplitude of the reference signal V_{ref} .

4.2 The Use of the Synchronous Detector for Extracting Signals Partially Correlated with the Probing Signal of the Electro-Acoustic Pickups

This use of the synchronous detector for the frequency

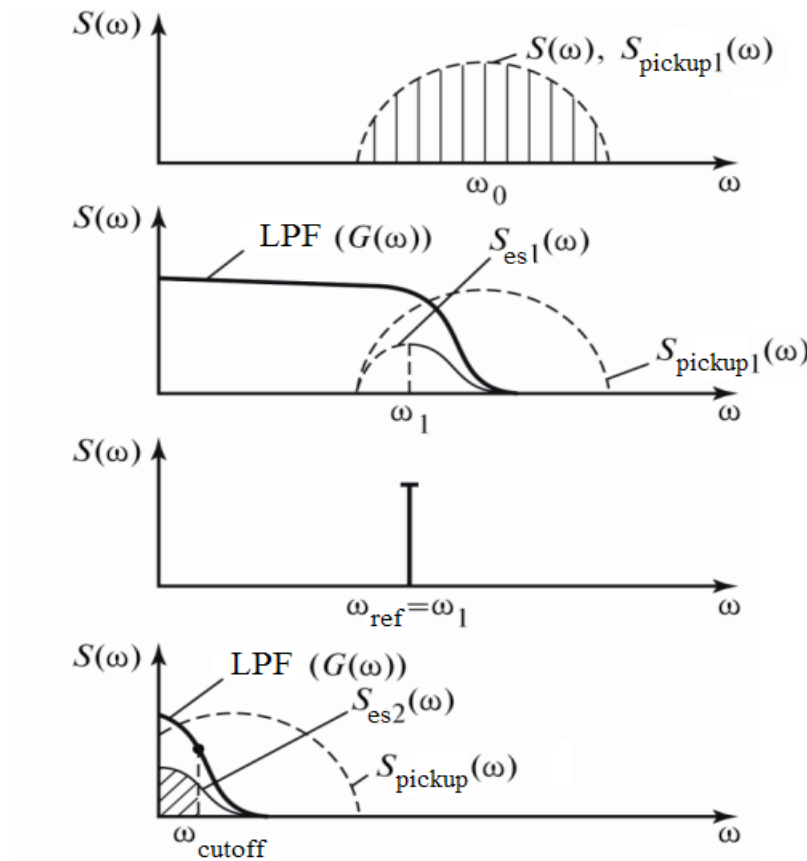


Figure 8. Suppression of the part of the EAP signal. (a) Spectrum of probing signal $S_{out}(\omega)$ and the corresponding spectrum EAP $S_{pickup}(\omega)$; (b) Spectrum of the echo signal $S_{es1}(\omega)$ at the output of product with a large attenuation of the US oscillations; (c) Spectrum of reference signal $\omega_{ref}=\omega_1$; (d) Spectrum signal $S_{es2}(\omega)$ at the output of LPF with a cutoff frequency ω_{cutoff}

separation of signal and interference allows suppressing not only narrow-band interference, but in some cases, it also enables the separation of the “useful” signal and the interference correlated with it for the purpose of partially suppressing the interference correlated with the probing signal. This possibility was realized for the partial suppression of the Electro-Acoustic Pickup (EAP) in the control of products with a large attenuation of ultrasound.⁵

Figure 8a shows the spectra of the probing signal $S(\omega)$ and the spectrum of the interference, the signal of the electroacoustic pickup $S_{pickup1}(\omega)$ coming from the emitting transducer to receive and mask the “useful” echo-signal. In this case, due to the large frequency-dependent attenuation, the spectrum of the signal radiated in the product $S(\omega)$ shown in Figure 8a undergoes severe distortion: the high-frequency components of the spectrum are attenuated to a greater extent than the low-frequency components. For this reason, the spectrum of the US echo signal $S_{es1}(\omega)$ differs from the spectrum of the emitted

signal $S(\omega)$: the maximum of the echo signal shown in Figure 8b) shifts to the frequency $\omega_1 < \omega_0$. Along with this, the spectrum of the electro-acoustic pickup $S_{pickup1}(\omega)$ is not distorted, $S_{pickup1}(\omega)$ in Figure 8b corresponds to the spectrum of the emitted signal $S(\omega)$ in Figure 8a.

In synchronous detection, the frequency of the reference signal $\omega_{ref} = \omega_1$ (Figure 8c) corresponding to the “shifted” maximum of the US echo signal ($\omega_1 < \omega_0$) is used, so due to the differences in the spectrum of the echo signal and the EAP spectrum, the echo signal $S_{es2}(\omega)$ enters the detector output virtually without any distortion (Figure 8d), and the major part of the electroacoustic pickup signal $S_{pickup}(\omega)$ is suppressed in the filter of low frequency $G(\omega)$. Thus, the signal/EAP ratio improves.

A structural diagram of the US flaw detector with suppression of the part of the EAP signal in the synchronous detector during the pulse echo control of products with a large attenuation of ultrasound is shown in Figure 9.

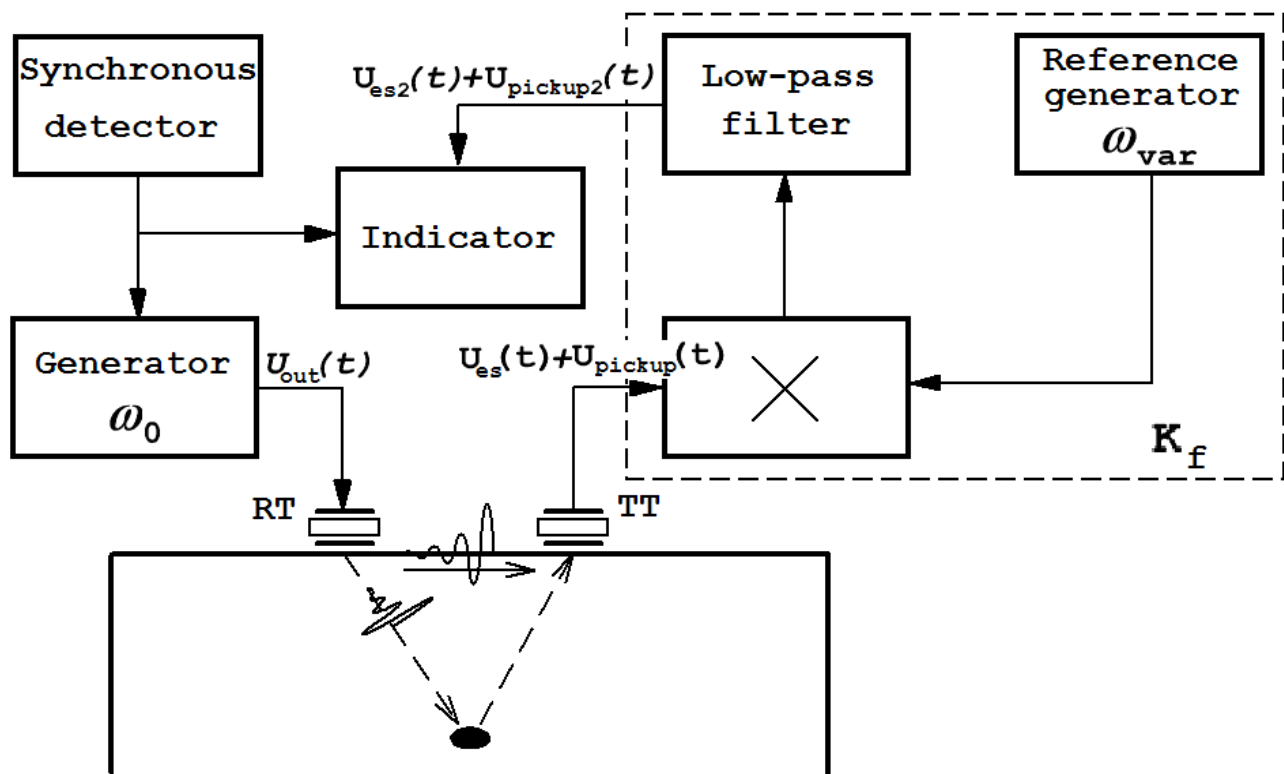


Figure 9. Structural diagram of the US flaw detector with suppression of the part of the EAP signal using the modified SD.

Strictly speaking, a modified diagram of the synchronous detector is used in the diagram in Figure 9, because the reference signal is not synchronous with the signal of the generator. Obviously, small deviations ω_{ref} and ω_1 occurring at the output of the diagram of beating will slightly worsen the result.

Finding the optimal parameters of the synchronous detector with the purpose of optimizing the echo/EAP ratio is also possible by selection of the parameters of LPF (cutoff frequency ω_{cutoff} and dip angle of AFC filter or, more generally, $\dot{E}_f(\omega)$ - LPF transfer constant). Let us

see the problem of choosing the optimal frequency ω_{cutoff} when using a probing signal with a duration of one period $T_s=T_o$ and frequency ω_o with spectral density $S_{out}(\omega)$. The

spectrum of such a signal can be written:

$$\dot{S}_{out}(\omega) = S_i \left[\frac{\sin \frac{(\omega - \omega_o)\dot{O}_s}{2}}{\frac{(\omega - \omega_i)\dot{O}_s}{2}} - \frac{\sin \frac{(\omega + \omega_o)\dot{O}_s}{2}}{\frac{(\omega + \omega_i)\dot{O}_s}{2}} \right] \tag{7}$$

The echo signal passing through an environment with frequency-dependent attenuation experiences a distortion of the spectrum, $S_{e1}(\omega) = \dot{S}_{out}(\omega) \dot{G}(\omega)$, where $\dot{G}(\omega) = G_o \exp(-\delta(\omega)x)$

is the frequency-dependent environment transfer rate, and G_o is a constant. The attenuation $\ddot{a}(\dot{u})$ for

definiteness is chosen as $\ddot{a}(\dot{u}) = \ddot{a}_1 \dot{u}^2$, where $\delta_o x =$

α is an integrated attenuation. At a fixed distance x , for the environment transfer rate, it will be:

$$\dot{G}(\omega) = G_o \exp(-\alpha \cdot \omega^2) \tag{8}$$

Distortion in the environment echo signal $\dot{S}_{est}(\omega)$ comes to the input of the filter with a transfer rate $\dot{E}(\omega)$

in the mixture with an EAP signal $\dot{S}_{pickup1}(\omega)$ correlated with the probing signal: $\dot{S}_{pickup1}(\omega) \approx \dot{S}_{out}(\omega)$. To

reduce the signal/ pickup ratio, it is necessary to synthesize the filter $\dot{E}_f(\omega)$ maximizing the ratio $q = \dot{S}_e(\omega) / \dot{S}_{pickup}(\omega)$. Obviously, this task is not statistical, but deter-

ministic. For definiteness, we will assume that the echo signal and EAP arrive at the filter at the same time. The task of construction of the filter is to obtain a maximum signal/ pickup ratio at the output of the filter:

$$q_2 = \frac{\left[\frac{\dot{S}_{e2}(\omega)}{\dot{S}_{pickup2}(\omega)} \right]}{\frac{\int_{-\infty}^{+\infty} |S_{e1}(\omega)| |K(\omega)| \dot{G}(\omega) d\omega}{\int_{-\infty}^{+\infty} |S_{e1}(\omega)| |K(\omega)| d\omega}} \tag{9}$$

For that, it is necessary to find $|K(\omega)|$ when q_2 is maxi-

mal. The criterion for selecting the LPF should be the condition of the maximum undistorted transmission of echo signal spectrum and the maximum suppression of the acoustic pickup spectrum. An LPF with a maximally flat AFC - Butterworth filter satisfies this condition. For the selected probing signal (section of sine wave with a duration of one period), let us calculate the dependence of the maximum relationship of the amplitude of the echo signal to the maximum value of the acoustic pickup at the output of the filter from a cutoff frequency $q_2 = f(\omega_{cutoff})$. To calculate, let us accept a signal/ pickup ratio at the input of the filter of $q_1=1$. The value of the environment transfer rate at frequency ω_o is assumed to be $G(\omega_o) = -20$ dB.

As a result of the calculation, the dependence $q_2 = f(\omega_{cutoff}/\omega_o)$ (Figure 10) is obtained, which shows that as the cutoff frequency decreases, the echo signal/EAP ratio increases by 2 times on average. On the same graph, the dashed line shows the dependence with less attenuation of the environment $G(\omega_o) = -10$ dB. The comparison

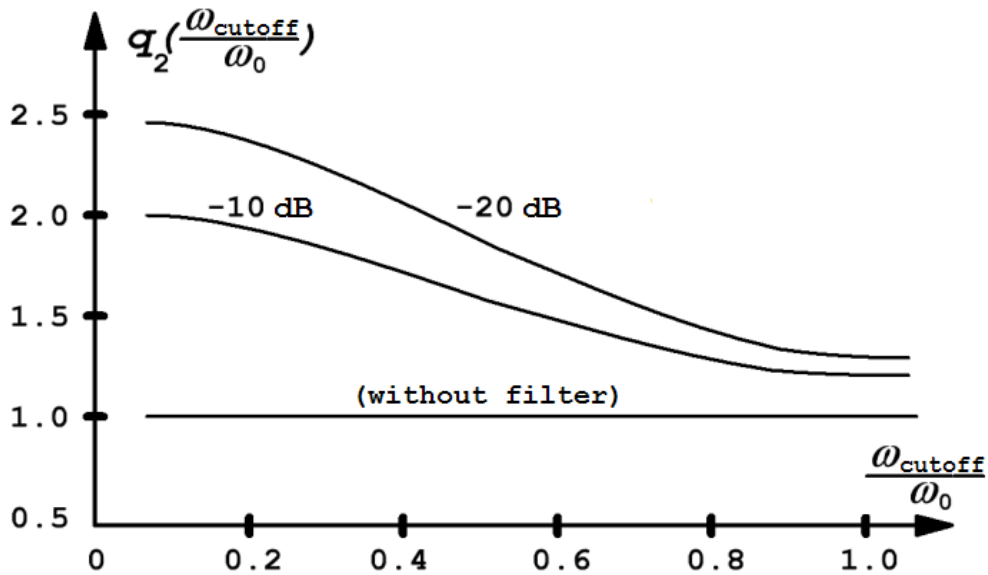


Figure 10. Dependence of the signal/acoustic pickup on the LPF cutoff frequency.

of the two curves shows that the effect of the suppression of acoustic pickup when using synchronous detection is stronger in environments with a greater attenuation of US oscillations (i.e., in environments with a stronger decorrelation of the echo signal and the EAP signal).

The effect of the acoustic pickup signal suppression in the time domain is shown in Figure 11. In the top graph, the signal of the acoustic pickup $V_{pickup1}(t)$ exceeded the echo signal $U_{es1}(t)$ by 3.5 times. After filtering (if $\omega_{cutoff} = 0,75\omega_0$), the pickup signal exceeds the echo signal only by 2 times⁶.

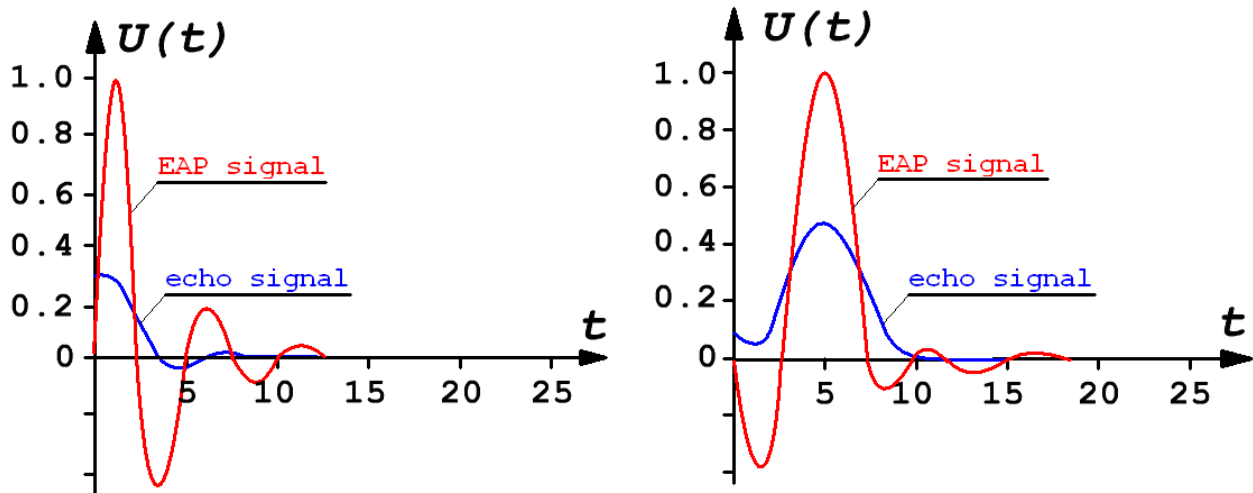


Figure 11. Amplitude of the EAP signals and the echo signal before (a) and after (b) LPF at $\omega_{av} = 0,75\omega_0$. $G(\omega_0) = -20$ dB.

5. Conclusion

Through the example of using synchronous detection in ultrasonic flaw detection, it can be observed that the use of the simplest radio-technical processing signals in the US control of products enables solving complex problems that cannot be solved in traditional flaw detection using simple unmodulated signals without additional processing.

6. Acknowledgment

The work was performed as part of the project "Organization of scientific research" at the base of the public tasks in the field of scientific work on the instructions of # 2014/123 for 2016.

7. References

1. Ermolov IN. Teoriya i praktika ul'trazvukovogo kontrolya [Theory and practice of ultrasonic testing]. Moscow: Mashinostroenie; 1981.
2. Kachanov VK, Sokolov IV. Application features of radio engineering signal processing methods for ultrasonic flow detection. *Nondestr Test Eval.* 2000; 15:330-60.
3. Kachanov VK, Sokolov IV. Features of applying complexly modulated signals in ultrasonic flaw detection. *Russian Journal of Non-Destructive Testing.* 2007; 12:18-42.
4. Kachanov VK, Sokolov IV, Rodin AB. Frequency separation of signals and interferences in noise-immune ultrasonic testing of articles manufactured from complexly structured materials. *Russian Journal of Non-Destructive Testing.* 2008; 11:21-30.
5. Kachanov VK, Pitolin AI, Ryabov GYu, Mozgovo AV, Kalugin PG. Sposob ul'trazvukovogo kontrolya izdelii s bol'shim zatukhaniem ul'trazvuka [Ultrasound testing technique for articles with high ultrasound damping]. Inventor's certificate RU 2006852. 1994.
6. Kachanov VK, Kartashev VG, Sokolov IV. Ul'trazvukovaya pomekhoustoichivaya defektoskopiya [Noise-immune ultrasonic testing]. Moscow: MPEI Press; 2007.